Application of fuzzy logic on CT-scan images of COVID-19 patients

Fariha Noor, Md. Rashad Tanjim, Muhammad Jawadur Rahim, Md. Naimul Islam Suvon, Faria Karim Porna, Shabbir Ahmed, Md. Abdullah Al Kaioum and Rashedur M. Rahman*

Department of Electrical and Computer Engineering,
North South University,
Plot-15, Block-B, Bashundhara,
Dhaka, Bangladesh
Email: fariha.noor@northsouth.edu
Email: rashad.tanjim@northsouth.edu
Email: jawadurrahim97@gmail.com
Email: naimul.suvon@northsouth.edu
Email: faria.porna@northsouth.edu
Email: shabbir.ahmed01@northsouth.edu
Email: abdullah.kaioum@northsouth.edu
Email: rashedur.rahman@northsouth.edu
*Corresponding author

Abstract: Image processing is crucial in any image analysis to determine the problem. If it is a medical area, a suitable image processing method becomes even more imperative to get as accurate results as possible. Due to the widespread outbreak of coronavirus disease 2019 (COVID-19), an infectious respiratory disease, it has become quite urgent that a reliable method for identification of the disease is sought. In this paper, we have segmented images with two different techniques, fuzzy *c*-means, and *k*-means clustering. Our images include CT-scan data and X-rays of both two categories. The first being the COVID-19 infected patients; the other being a collection of normal persons, and viral pneumonia infected persons. Among the two clustering techniques, the *k*-means performed better. Later, we trained our CNN model with the segmented images and raw images. Interestingly, the segmented images of CT-scan, as well as X-rays, are performing well in CNN classification rather than raw images. After applying fuzzy edge detection, the segmentation was improved. The f1-score for our model is 91% and the support is 89%.

Keywords: medical image processing; fuzzy *c*-means clustering; image segmentation; convolutional neural network.

Reference to this paper should be made as follows: Noor, F., Tanjim, M.R., Rahim, M.J., Suvon, M.N.I., Porna, F.K., Ahmed, S., Al Kaioum, M.A. and Rahman, R.M. (2021) 'Application of fuzzy logic on CT-scan images of COVID-19 patients', *Int. J. Intelligent Information and Database Systems*, Vol. 14, No. 4, pp.333–348.

Biographical notes: Fariha Noor recently completed her undergraduate in Computer Science and Engineering from North South University, with a minor in Artificial Intelligence. Her research interest lies in applying machine learning models to solve real-life problems. Recently, she has co-authored a conference paper on data mining. She has also worked with agent-based modelling simulation. Currently, she is working on a project in human activity detection using digital imaging. Besides researching, she likes to travel and read books.

Md. Rashad Tanjim is a Full-Stack developer having two years of freelancing experience in the field of developing and designing apps and websites. Recently, he has completed graduation on BS in Computer Science and Engineering from North South University, Dhaka, Bangladesh. Additionally, his areas of interest are machine learning and cloud computing. Currently, he is working as a software developer and developing industry level projects such as e-commerce apps and websites. Besides, he has research experience in artificial intelligence and he has already co-authored in two conference papers and one journal paper in this field.

Muhammad Jawadur Rahim has recently completed his undergraduate from North South University, Dhaka. Currently, he is working at a startup focused on making machine learning models more accessible for people without coding skills. He has experimented and researched on the simulation of agent-based modelling and different pattern recognising techniques. His research endeavours extend toward GAN to reconstruct famous paintings. He is also working on retrofitting models to compute image analysis onboard embedded systems by eliminating the need for cloud computing and data routing.

Md. Naimul Islam Suvon is a Computer Science and Engineering student at North South University, Bangladesh. His future goal is to secure a challenging position in a reputable institution to expand his research, knowledge, and skills. His research interests are in deep learning, machine learning, data mining, and computer vision.

Faria Karim Porna is currently a last semester student of North South University. She is doing her major in CSE from the ECE department of this university. Her areas of interests are fuzzy system, artificial intelligence, computer vision and image processing on medical images. She has also interest in mathematical problems in the domain of differential equations and power series.

Shabbir Ahmed is currently pursuing his Bachelor of Science in Computer Science and Engineering at North South University. He is doing his last year's senior research on applying machine learning techniques in remote sensing and agriculture. His research interest includes fuzzy logic, remote sensing, applying machine learning models, and digital ethics.

Md. Abdullah Al Kaioum is a fourth-year undergraduate student of Computer Science and Engineering in the School of School of Engineering and Physical Sciences at the North South University, in Dhaka, Bangladesh. His research interests include artificial intelligence, cloud computing, information security and technology innovation, wireless networking, databases and data mining.

Rashedur M. Rahman is working as a Professor in Electrical and Computer Engineering Department, North South University, Dhaka, Bangladesh. He received his PhD in Computer Science from University of Calgary, Canada. He has authored more than 150 peer-reviewed research papers. His current research interests are in data science, cloud load characterisation, optimisation of cloud resource placements, deep learning, etc.

1 Introduction

Computer-aided medical treatment has been used since the 1930s, first with the electroconvulsive therapy (ECT) and now with robot-assisted surgery. The quality of the tests and analysis is much more superior to what it was before. With the success that has come from using the computer-aided medical treatment, more and more study has been done to grasp the extent to which computers can provide proper medical assistance. One of such fields where artificial intelligence is being used relentlessly is in the analysis of biomedical images and then computing an accurate result. For that, it is necessary to process various biomedical images using different techniques, including, but not limited to, skeletonisation, segmentation, clustering. Processing medical images, such as X-rays, magnetic resonance imaging (MRI), etc. is an essential introductory step to obtain precise results. Hence, more importance is given to how the medical images are pre-processed.

Figure 1 Flow diagram of the proposed system

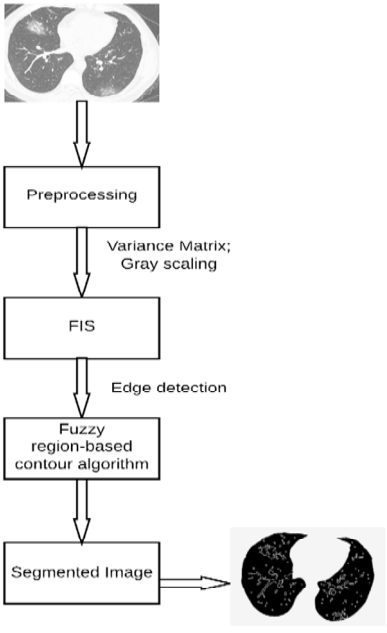

There are some major characteristics of a CT scan that can tell us more about the patients' respiratory illness. The main features of a CT scan are ground-glass opacity, consolidation, crazy-paving pattern. In radiology, ground-glass opacity is an observation

on computed tomography (CT) scans that indicates a partial filling of air spaces by exudate or transudate, as well as an interstitial thickening or partial lung alveoli collapse. In CT scans, it appears to be cloudy. Consolidation is a type of airspace disease that causes the filling of the alveolar spaces. In a CT scan, it appears to have indistinct margins and it presents as fluffy opacities that become confluent over time. Crazy paving patter is the scattered or diffuse ground-glass attenuation with superimposed interlobular septal thickening and intralobular lines. On analysis of the CT scan images, it is found that about 61.3% of the patients had ground-glass opacity, about 35.5% of patients had ground-glass opacity with consolidation, and 25.8% had a crazy-paving pattern (Zhou et al., 2020). The outbreak of COVID-19 was first discovered and identified in viral pneumonia cases that arose in Wuhan (Jin et al., 2020). It is an infectious disease. The fact that it is also highly contagious, has made it incredibly difficult to tackle. As of 12 June 2020, the total cases of COVID-19 are of 7,550,427 confirmed cases in 215 countries, with 421,893 confirmed deaths [Who Coronavirus Disease (COVID-19) Dashboard, https://covid19.who.int/]. Figure 1 shows the working methodology for the paper.

We have taken the CT scan images and X-ray images of COVID-19 infected patients as our dataset. Our dataset also consists of CT-scans and X-rays of persons who were not affected by COVID-19. That means the second class of our images also included patients having viral and bacterial pneumonia. We were able to collect our data from four different sources and later we merged it to create a unique dataset consisting of 2,041 images in total. We had to remove some totally distorted images. Moreover, the images are then augmented 180°, and finally, we obtain 2,041 images. Our goal is to segment the images using thresholding, clustering, and edge detection algorithm and then feed the images to CNN to see which images give the best result. For segmentation, we use fuzzy *c*-means (Çetin et al., 2019; Fang et al., 2019) and the *k*-means clustering algorithm (Dhanachandra et al., 2015). For edge detection, we used fuzzy logic edge detection (Dhargupta et al., 2019), canny, sobel, and log. We wanted to perform a comparison and analysis between the segmentation techniques to see which one works better. Our main focus is not on the segmentation technique but rather on classifying the COVID-19 infected and non-infected person using the said segmented images.

2 Literature review

Huang et al. (2019) combined fuzzy means clustering and rough set theory and proposed a new technique for segmenting the image. At first, they segmented the brain CT scan using a fuzzy *c*-means clustering algorithm. The images were separated into different parts depending on the relationship of attributes. The value of the segmentation is determined and the brain image is again generated artificially. The authors showed that this methodology not only reduced the error rate but also performed better segmentation. This technique also appeared to be noise-resistant.

Jiang et al. (2020) worked with brain CT images, to segment it under different conditions. Medical images are taken using different machines, different patients, and in different conditions. Most of the time, medical images are distorted with noises. Different segmentation works well for noise-free images. The authors have introduced a technique of processing and segmenting brain CT scans by applying a varying degree of noise.

They have proposed a negative transfer-resistant fuzzy clustering model that was able to segment images, even under the presence of noise. Their approach is similar to ours as we have worked with the CT scan images by segmenting it using different techniques.

Sharma (2020) have discussed the role of machine learning techniques for getting important insights like whether lung CT scan be the first screening/alternative test for real-time reverse transcriptase-polymerase chain reaction (RT-PCR) and whether COVID-19 pneumonia is different from other viral pneumonia. Ground-glass opacities (GGO), consolidation, and pleural effusion are the three predominant features they have concentrated to distinguish COVID-19 pneumonia from other viral pneumonia. The research had used custom vision software based on the ResNet architecture of Microsoft azure for the training purposes. The authors built their database of almost 2,200 images. After training and testing the model, about 91% accuracy was reported. From their research, they have found that pneumonia due to coronavirus tends to affect all of the lungs, instead of just small parts and coronavirus shows a typical patch on the outer edges of the lungs.

Varieties of works have been conducted to optimise using an evolving deep convolutional neural network to develop a better CNN model. In this purpose, Sun et al. (2019) proposed a method using genetic algorithms for evolving the architectures and connection weight initialisation values of a deep convolutional neural network to address image classification problems where an efficient variable-length gene encoding strategy was designed to represent the different building blocks and the potentially optimal depth in convolutional neural networks. Their target was to achieve a new weight initialisation strategy and a new coding scheme. In our paper, we have also used a pre-tainted ImageNet model and done fine-tuning to achieve greater accuracy.

Xu et al. (2019) worked on extracting the cancerous tissues of the breast using image segmentation. For image segmentation, they used CNN to extract four different types of issues related to breast cancer. As a dataset, they worked on 3D breast ultrasound images. The evaluation of the segmentation gave good results, over 80%, and a Jaccard similarity index of 85.1%. This might be useful in classifying and dragonising breast ultrasound images.

3 Dataset collection

The most important part of any machine learning experiment is its data and its source. At the time of the experiment, no one source had a sufficient number of images. Hence, we collected the images from different online sources and built our new unique dataset. Our dataset contains the image from the Italian Society of Radiology (SIRM) (COVID-19 Database, https://www.sirm.org/en/category/articles/covid-19-database). We were also able to obtain images of COVID-19 infected and non-infected persons from the Kaggle repository (SARS-CoV-2 CT-Scan Dataset, https://www.kaggle.com/plameneduardo/sarscov2-ctscan-dataset) and an online repository (Rahimzadeh et al., 2020). For pneumonia, we collected it from the website (Pneumonia, https://radiopaedia.org/search?lang=us&q=pneumonia&scope=cases).

Figure 2 Variance matrix calculation

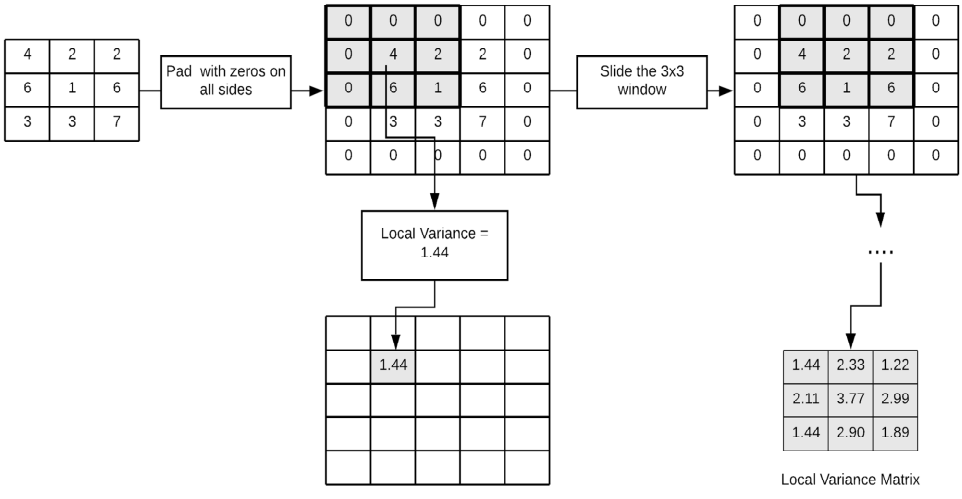

4 Methodology

The CT scanner differs from X-ray in the way that X-rays only use one radiation beam, whereas CT scanners use a series of narrow beams to produce a more refined final picture. On examining the CT scan images, the tender tissues, bone, fat and gaseous substance would be represented in a different hue. Any abnormality can be detected by identifying an unexpected colour. We want to create a model that would be able to classify the disease by examining the lung CT scan.

For the model to be able to work on the images, it has to be pre-processed for increasing the probability of correct results. The images obtained are RGB, that is, an m-by-n-by three data matrices. The images are converted to greyscale images, which is a dimensional matrix for the model to segment correctly. After the conversion, the variance matrix is determined to localise the affected area of the lungs. After that, we have applied both fuzzy *c*-means, *k*-means, and thresholding algorithms separately to segment the images. We have also applied four different edge detection techniques to improve the segmentation. Though we have segmented the images using three algorithms, we use only two segmentation for classification because we want to compare and analyse between fuzzy *c*-means and *k*-means algorithm to get the best of them. To better evaluate our segmentation, we have used CNN models to classify the segmented images. Instead of using the basic CNN model, we have made different adjustments to the model and performed classification.

4.1 Determining the variance matrix

We have computed the variance matrix by determining the local variance of the greyscale converted image. Moreover, we define a window of size 3 × 3 that will calculate the local mean of a pixel by averaging the surrounding pixels. The image matrix is padded with zeros on all sides. The local mean is calculated by sliding the 3 × 3 window on the

matrix. The middle value is replaced with the mean. The process is repeated for all the elements in the matrix. The matrix obtained at the end is the variance matrix, which localises the affected area (Woźniak et al., 2018). The local variance is computed by:

$$\text{var}\left(I_{x,y}\right) = E\left[\left(I_{x,y}\right)^2\right] - \left(E\left[I_{x,y}\right]\right)^2 \tag{1}$$

In equation (1), $I_{x,y}$ is the matrix of the greyscale image, $E[(I_{x,y})]^2$ is the local mean of $(I_{x,y})^2$ and $(E[I_{x,y}])^2$ is the [local mean of $(I_{x,y})$]^2. Figure 2 shows the variance matrix calculation

4.2 Edge detection using FIS

After the variance matrix is obtained, we have identified the affected areas. We need to bind the areas with an edge for easier segmentation. For edge detection, we need to determine two uniform regions by comparing the intensity of the surrounding pixels. However, the uniform areas are not strictly crisp because the intensity of the neighbouring pixels might not always represent an edge. To avoid this problem, the fuzzy system can be used where some degree of impreciseness can be allowed. Figure 3 depicts the fuzzy inference model.

Figure 3 Fuzzy inference system

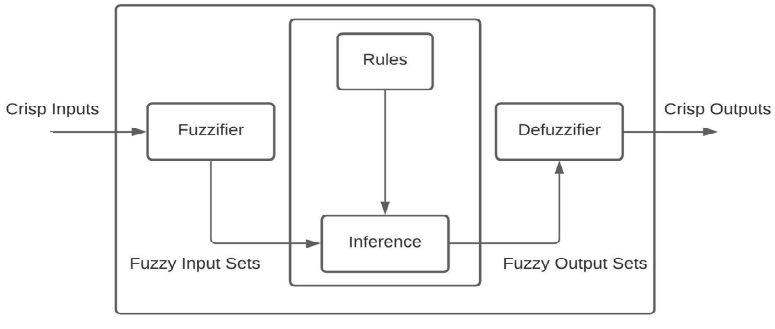

4.2.1 Defining a linguistic variable

At first, the image gradient is computed. The image gradient will be our crisp input. The fuzzy edge detection method depends on the values of the image gradient. To compute the image gradient, we use the following formula:

$$\Delta f = \begin{bmatrix} g_x \\ g_y \end{bmatrix} = \begin{bmatrix} \frac{\partial f}{\partial f} \\ \frac{\partial f}{\partial y} \end{bmatrix} \tag{2}$$

where

- $\frac{\partial f}{\partial x}$ is the gradient along the x-axis

- $\frac{\partial f}{\partial y}$ is the gradient along the y-axis.

Here, $\frac{\partial f}{\partial y}$ is calculated by applying the 1-dimensional filter to the image $I_{x,y}$ using convolution.

$$\frac{\partial f}{\partial y} = \begin{bmatrix} -1 \\ +1 \end{bmatrix} * I_{x,y} \tag{3}$$

Hence, the gradients g_x and g_y of the image act as the crisp input to our model, which now we need to convert it to fuzzy values using the membership function.

4.2.2 Input fuzzification

As the input of our model has crisp value, we can define the membership function as μ function for each input. The membership functions are:

$$\mu_A i(x) = \exp\left(-\frac{(c_i - x)^2}{2\sigma_i^2} \right) \tag{4}$$

Here, c_i is the centre and σ_i is the width of the fuzzy set A^i.

The membership function selected for fuzzification is a Gaussian function, also known as normal distribution. Hence, the function acts as a zero-mean Gaussian function. For the pixels having values of 0, it belongs to the membership function with a degree of 1. We set the standard deviation for the membership function selected for fuzzification is a Gaussian function, also known as normal distribution. Hence, the function acts as a zero-mean Gaussian function. For the pixels having values of 0, then it belongs to the membership function with a degree of 1. We set the standard deviation for the membership function as the hyperparameter for the inputs. If the standard deviation is higher, then the algorithm becomes less perceptive in detecting the edges. On the other hand, if the standard deviation is lower, then the intensity of the detected edges will be lower. Figure 4 shows the plot of the membership function for input values.

4.2.3 Fuzzy model

After defining the membership function, we can now define the rules of our system. For a pixel to classify as an edge, we have to set a value to it. The fuzzy rules are:

Rule 1 If the pixel is 1, then the output value will be white.

Rule 2 If the pixel is 0, then the output is not 1, so the output will be black.

4.2.4 Defuzzification

For defuzzification, we need to set another membership function for our output values. For this, we define a triangular function.

Equation (5) is our membership function for output values.

$$\mu_A(x) = \begin{cases} 0 & \text{if } x \le a \\ \dfrac{x-a}{b-a} & \text{if } a \le x \le b \\ \dfrac{c-x}{c-b} & \text{if } b \le x \le c \\ 0 & \text{if } x \ge c \end{cases} \tag{5}$$

Here, a, b and c are the three vertices of the triangle. Figure 5 shows the plot of the membership function for output values. As we have defined our membership functions and the rules of our model, we detect edges using the model. The defuzzification technique used is the middle of maximum (MOM). We have set the membership function in such a way that, if the pixel value is 1, the pixel will belong to white with a membership degree of 1 and the pixel will belong to black with a degree of 0. Again, if the pixel value is 0, it will belong to white with a membership degree of 0 and it will belong to black with a degree of 1. Here, we give a lot of emphasis on edge detection because we will segment these images and use them as our input to the CNN model. In our project, we have used four different edge detection techniques to determine which gives the best result.

Figure 4 Input fuzzification (see online version for colours)

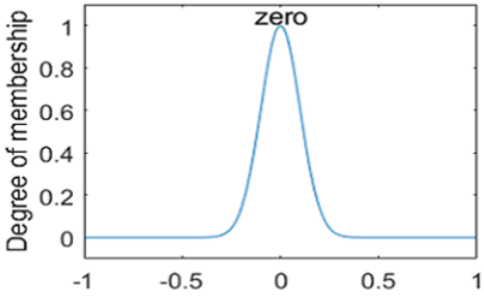

Figure 5 Membership function for output values (see online version for colours)

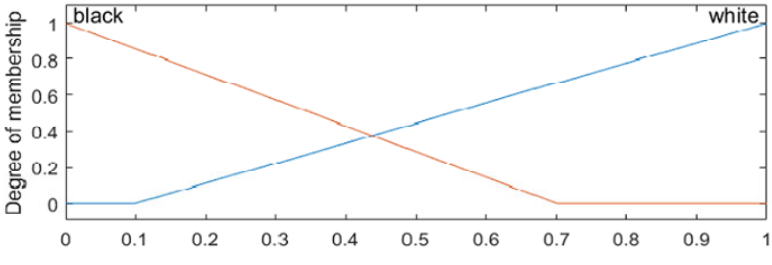

4.3 Segmenting the images

For our image segmentation, we have used four methods. First by thresholding the image, second by *k*-means clustering and then by fuzzy *c*-means clustering, and finally by edge detection. For our edge detection part, we have applied fuzzy edge detection, canny,

sobel, and log technique. The images are evaluated by comparing it with the ground truth images. We have shown a comparison and contrast between the different edge detection algorithms to show which one gives the best performance. Figure 6 shows the result of the different segmentation of the original image.

Figure 6 (a) Original COVID image (b) Segmented image using fuzzy *c*-means (c) Segmented images using *k*-means (d) Thresholding (see online version for colours)

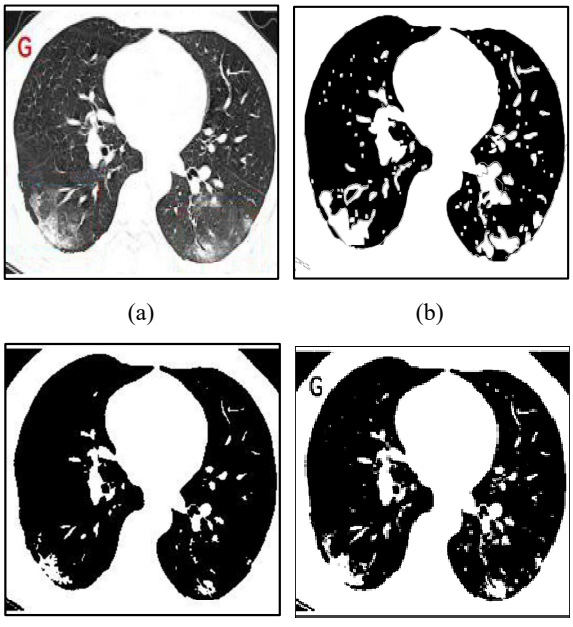

Figure 7 Final model diagram of the different layers of CNN (see online version for colours)

4.4 CNN model

Different CNN architecture performs better in image classification. We have used five different models and among them a pre-trained VGG16 with data augmentation and fine-tuning works best in this regard.

In the output layers, the model has in total 20,221,249 parameters among them 18,485,761 parameters are trainable and 1,735,488 parameters are non-trainable. Sigmoid as activation function and Binary cross-entropy as loss function has been used. The VGG16 model has (1,600, 10,240) train bottleneck features and (400, 10,240) validation bottleneck features.

Figure 7 shows the final model diagram of the different layers.

5 Results and discussion

For, our thresholding methodology, we have made our own custom threshold method which is different from Otsu's (1979) thresholding. Whereas Otsu's method is adaptive and determines the optimal threshold value by evaluating the input image, in our paper we have set the threshold value to 200 for all images. After some test and trial, we found that setting the value to 200 produces the best segmentation results. To evaluate the image segmentation, we need a ground-truth image. For our paper, the Otsu's imbinarise method in MATLAB is used to produce the ground-truth image from raw image. We apply fuzzy *c*-means, *k*-means and our modified version of thresholding to the raw images individually. Tree obtained images are then compared with our ground-truth image that we obtained using the Otsu's method separately. The standard metrics used for image segmentation are dice overlap coefficient and Jaccard index. These metrics measure the similarity between the obtained segmentation and the desired output segmentation. For the segmentation, we have considered the following metrics. Table 1 shows the evaluation of the segmented image with respect to the ground truth image.

Table 1 Evaluation of different segmentation technique

	Fuzzy c-means	*K-means*	*Thresholding*
True positive	0.49	0.49	0.51
True negative	0.38	0.49	0.49
False positive	0.11	0.002	0.0005
False negative	0.02	0.026	0.002
Accuracy	0.87	0.97	0.997
F-measure	0.88	0.97	0.997
Precision	0.82	0.99	0.999
Recall	0.95	0.95	0.996
Specificity	0.78	0.99	0.998
Jaccard similarity index	0.79	0.94	0.994
Dice similarity	0.88	0.97	0.997
Matthews correlation coefficient	0.75	0.944	0.994

From Table 1, we see that the best segmentation is done by *k*-means clustering and thresholding. Both *k*-means and thresholding give very close results. However, the f-measure and Jaccard similarity index are highest for thresholding, about 0.997 and 0.994 respectively. Fuzzy *c*-means performs the least segmentation among the three. The Jaccard similarity index and dice similarity are about 0.79 and 0.88 respectively for fuzzy *c*-means clustering.

Table 2 Evaluation of different edge detection technique

	Fuzzy edge	*Canny*	*Sobel*	*Log*
True positive	0.488	0.01	0.01	0.013
True negative	0.038	0.41	0.47	0.44
False positive	0.449	0.079	0.02	0.043
False negative	0.024	0.502	0.502	0.49
Accuracy	0.53	0.42	0.47	0.47
F-measure	0.67	0.034	0.038	0.046
Precision	0.52	0.115	0.33	0.23
Recall	0.95	0.02	0.02	0.025
Specificity	0.078	0.84	0.96	0.91
Jaccard similarity index	0.507	0.017	0.019	0.023
Dice similarity	0.67	0.03	0.038	0.046
Matthews correlation coefficient	0.06	–0.25	–0.066	–0.14

The best is performed by fuzzy edge detection, which gives an accuracy of 0.53. Only fuzzy edge detection has a positive MCC. Canny, sobel, and log gave an MCC of less than 0.

For our next step of the methodology, we use the segmented images that we obtained from fuzzy *c*-means clustering and *k*-means clustering. We have tried seven different models for our classification.

Table 3 shows the accuracy of CNN in classifying *k*-means segmented images.

Table 3 Classifying *k*-means segmented images

SL.	*Name*	*Train loss*	*Train accuracy*	*Validation loss*	*Validation accuracy*
1	Basic CNN layers	0.0036	0.99	1.636	0.7875
2	CNN with dropout layers	0.0640	0.98	2.0674	0.8025
3	CNN with dropout layers using data augmentation	0.4010	0.8174	0.4904	0.8290
4	Basic transfer learning	0.0238	0.9924	3.841	0.808
5	Using data augmentation with re-scaling	0.33	0.8495	4.139	0.8110
6	Pre-trained CNN with data augmentation and fine tuning	0.0213	0.9919	0.3486	0.9690

The model confusion matrix denotes the true positive rate and false positive rates.

Table 4 Model performance metrics and prediction confusion matrix

Accuracy	*Precision*	*Recall*	*F1-score*	*Support*
0.96	0.90	0.91	0.91	0.89

The model confusion matrix denotes the true positive rate and false positive rates.

The false positive rates are lower and by analysing the table it is denoted that the model works well in classifying between COVID patients and non-COVID patient's segmented CT-scan images. We have tested 50 unseen images including 20 COVID patients to the models. Figure 8 shows the receiver operating curve (ROC) of the clustering models.

Figure 8 Receiver operating curve (ROC) of the CNN model of fuzzy *c*-means and *k*-means clustering model (see online version for colours)

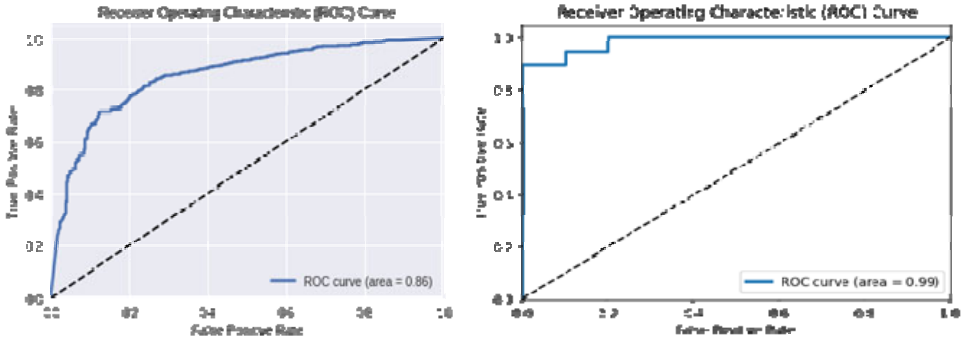

Figure 9 shows the accuracy and loss graph of the model.

Figure 9 Basic CNN performance evaluation *k*-means segmented image (see online version for colours)

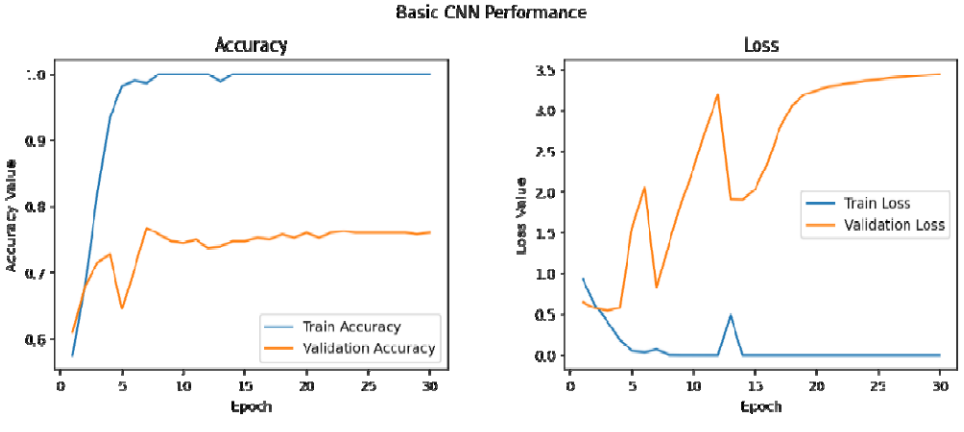

The highest validation accuracy that we obtain from the *k*-means segmented image is about 97%. If we analyse the graph of basic CNN layers, we see that although the training accuracy is almost 99%, the validation accuracy is barely 79%. For a good model, the training accuracy and validation accuracy has to be somewhat close to each

other. But in our case, the basic CNN model does not give the best performance. We then experiment with different models and the best output was obtained from pre-trained CNN with data augmentation and fine-tuning, where the validation accuracy and training accuracy are very close to each other. So, some adjustments to the CNN model performs much better than the basic model. We think if we have increased the number of images in the dataset, we will get better performance from the model.

Next, we applied the same model but, in this case, we have used the fuzzy segmented images as input. Table 5 shows the accuracy of CNN in classifying fuzzy *c*-means segmented images.

Table 5 Classifying fuzzy *c*-means segmented images

SL.	*Name*	*Train loss*	*Train accuracy*	*Validation loss*	*Validation accuracy*
1	Basic CNN layers	0.0000	1.00	3.1361	0.7725
2	CNN with dropout layers	0.0157	0.993	1.8956	0.7550
3	CNN with dropout layers using data augmentation	0.5099	0.7490	0.6288	0.6960
4	Basic transfer learning	0.0373	0.9887	0.4865	0.8650
5	Using data augmentation with re-scaling	0.4211	0.7966	0.5257	0.8150
6	Pre-trained CNN with data augmentation and fine tuning	0.0727	0.9764	1.1641	0.8730

Figure 10 shows the graph of the basic CNN model accuracy and loss.

Figure 10 Basic CNN performance evaluation for fuzzy segmented images (see online version for colours)

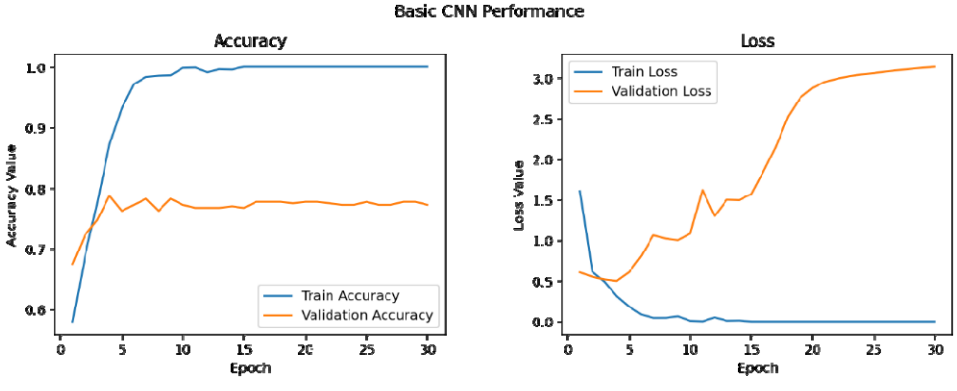

For the fuzzy segmented images, we observed a similar pattern like that of the *k*-means. Just like *k*-means, the basic CNN model for the fuzzy segmented images performed poorly. Where the training accuracy is 100%, the validation accuracy is only 77%. We have classified the images using different variations of the same model. We observe in the case of fuzzy segmented images, the best performance is given by pre-trained CNN with data augmentation and fine-tuning, where the training accuracy is about 98% and the validation accuracy was about 87%, even though the performance was not as good as the *k*-means segmented images.

Pre-trained CNN with data augmentation can classify the *k*-means segmented image with greater accuracy. This could be due to the fact that the images are segmented properly with *k*-means. Moreover, in fuzzy *c*-means, those boundary points are not taken into account, whereas in *k*-means some boundary points were clustered which gave better results when it is evaluated. Furthermore, the pre-trained CNN with data augmentation and fine-tuning model's train and test accuracy has a slight difference which also indicates that this model is better than the fuzzy *c*-means model. A limitation of the research is that we have a smaller number of images. For a CNN model, the greater the dataset, the greater is the performance. Since our scope is only limited to COVID-19, we have to work with a smaller dataset. Moreover, all the images are not of good quality and the same dimension. Some images have been discarded because they are completely distorted.

6 Conclusions

In this paper, we have segmented lung CT scan images and X-rays of COVID-19 infected persons and non-infected persons which is then classified by CNN. For segmentation, we have applied fuzzy *c*-means clustering, *k*-means clustering algorithm, and thresholding. We have also applied edge detection techniques. In classification, the segmented images using *k*-means performs better than the fuzzy *c*-means clustering because the segmentation of *k*-means is of good quality. We want to compare the *k*-means segmentation and fuzzy *c*-means segmentation and the result shows that *k*-means clustering performed better in segmentation. Though the basic CNN models do not perform as expected, a slight variation gives much better results for both the fuzzy *c*-means clustering and *k*-means clustering. In the future, we want to further enhance this model so that it can classify different diseases, not just COVID-19. We plan to include a greater number of images for classification. We believe aid in artificially diagnosing diseases.

References

Çetin, M., Dokur, Z. and Ölmez, T. (2019) 'Fuzzy local information c-means algorithm for histopathological image segmentation', in *2019 Scientific Meeting on Electrical-Electronics & Biomedical Engineering and Computer Science (EBBT)*, IEEE, pp.1–6.

COVID-19 Database [online] https://www.sirm.org/en/category/articles/covid-19-database (accessed 1 May 2020).

Dhanachandra, N., Manglem, K. and Chanu, Y.J. (2015) 'Image segmentation using *k*-means clustering algorithm and subtractive clustering algorithm', *Procedia Computer Science*, Vol. 54, pp.764–771.

Dhargupta, S., Chakraborty, A., Ghosal, S.K., Saha, S. and Sarkar, R. (2019) 'Fuzzy edge detection based steganography using modied Gaussian distribution', *Multimedia Tools and Applications*, Vol. 78, No. 13, pp.17589–17606.

Fang, J., Liu, H., Zhang, L., Liu, J. and Liu, H. (2019) 'Fuzzy region-based active contours driven by weighting global and local fitting energy', *IEEE Access*, Vol. 7, pp.184518–184536.

Huang, H., Meng, F., Zhou, S., Jiang, F. and Manogaran, G. (2019) 'Brain image segmentation based on FCM clustering algorithm and rough set', *IEEE Access*, Vol. 7, pp.12386–12396.

Jiang, Y., Gu, X., Wu, D., Hang, W., Xue, J., Qiu, S. and Chin-Teng, L. (2020) 'A novel negative-transfer-resistant fuzzy clustering model with a shared cross-domain transfer latent space and its application to brain CT image segmentation', *IEEE/ACM Transactions on Computational Biology and Bioinformatics*.

Jin, Y-H., Cai, L., Cheng, Z-S., Cheng, H., Deng, T., Fan, Y-P., Fang, C., Huang, D., Huang, L-Q., Huang, Q. et al. (2020) 'A rapid advice guideline for the diagnosis and treatment of 2019 novel coronavirus (2019-nCoV) infected pneumonia (standard version)', *Military Medical Research*, Vol. 7, No. 1, p.4.

Otsu, N. (1979) 'A threshold selection method from gray-level histograms', *IEEE Trans. Sys. Man. Cyber*., Vol. 9, No. 1, pp.62–66, DOI: 10.1109/TSMC.1979.4310076.

Pneumonia [online] https://radiopaedia.org/search?lang=us&q=pneumonia&scope=cases (accessed 1 May 2020).

Rahimzadeh, M., Attar, A. and Sakhaei, S.M. (2020) *A Fully Automated Deep Learning-Based Network for Detecting COVID-19 from A New and Large Lung CT Scan Dataset*, medRxiv.

SARS-CoV-2 CT-Scan Dataset [online] https://www.kaggle.com/plameneduardo/sarscov2-ctscan-dataset (accessed 1 May 2020).

Sharma, S. (2020) 'Drawing insights from COVID-19-infected patients using ct scan images and machine learning techniques: a study on 200 patients', *Environmental Science and Pollution Research*, pp.1–9.

Sun, Y., Xue, B., Zhang, M. and Yen, G.G. (2019) 'Evolving deep convolutional neural networks for image classification', *IEEE Transactions on Evolutionary Computation*, Vol. 24, No. 2, pp.394–407.

Who Coronavirus Disease (COVID-19) Dashboard [online] https://covid19.who.int/ (accessed 9 May 2020).

Woźniak, M., Połap, D., Capizzi, G., Sciuto, G.L., Kośmider, L. and Frankiewicz, K. (2018) 'Small lung nodules detection based on local variance analysis and probabilistic neural network', *Computer Methods and Programs in Biomedicine*, Vol. 161, pp.173–180, doi: 10.1016/j.cmpb.2018.04.025.

Xu, Y., Wang, Y., Yuan, J., Cheng, Q., Wang, X. and Carson, P.L. (2019) 'Medical breast ultrasound image segmentation by machine learning', *Ultrasonics*, Vol. 91, pp.1–9.

Zhou, Z., Guo, D., Li, C., Fang, Z., Chen, L., Yang, R., Li, X. and Zeng, W. (2020) 'Coronavirus disease 2019: initial chest CT findings', *European Radiology*, pp.1–9.